Chemistry–A European Journal
Research Article
doi.org/10.1002/chem.202301325
Chemistry Europe
European Chemical Societies Publishing

www.chemeurj.org

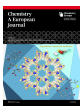

Degradation of Penicillinic Antibiotics and β-Lactamase Enzymatic Catalysis in a Biomimetic Zn-Based Metal–Organic Framework

Paula Escamilla[+],[a] Lucia Bartella[+],[b, c] Sergio Sanz-Navarro[+],[d] Rita Maria Percoco,[b] Leonardo Di Donna,[b, c] Mario Prejanò,[b] Tiziana Marino,[b] Jesús Ferrando-Soria,*[a] Donatella Armentano,*[b] Antonio Leyva-Pérez,*[d] and Emilio Pardo*[a]

Abstract: β-Lactam antibiotics are one of the most commonly prescribed drugs to treat bacterial infections. However, their use has been somehow limited given the emergence of bacteria with resistance mechanisms, such as β-lactamases, which inactivate them by degrading their four-membered β-lactam rings. So, a total knowledge of the mechanisms governing the catalytic activity of β-lactamases is required. Here, we report a novel Zn-based metal–organic framework (MOF, **1**), possessing functional channels capable to accommodate and interact with antibiotics, which catalyze the selective hydrolysis of the penicillinic antibiotics amoxicillin and ceftriaxone. In particular, MOF **1** degrades, very efficiently, the four-membered β-lactam ring of amoxicillin, acting as a β-lactamase mimic, and expands the very limited number of MOFs capable to mimic catalytic enzymatic processes. Combined single-crystal X-ray diffraction (SCXRD) studies and density functional (DFT) calculations offer unique snapshots on the host-guest interactions established between amoxicillin and the functional channels of **1**. This allows to propose a degradation mechanism based on the activation of a water molecule, promoted by a Zn-bridging hydroxyl group, concertedly to the nucleophilic attack to the carbonyl moiety and the cleaving of C–N bond of the lactam ring.

Introduction

β-Lactam antibiotics -including penicillins, cephalosporins and cephamycins, monobactams, carbapenems and carbacephems- are the most commonly used group of antibiotics against bacterial infections.[1] They all have in common the presence of a four-membered β-lactam ring in their chemical structure, which lies at the origin of their antibacterial properties.[1] However, this feature also represents the main drawback of this family of antibiotics as certain bacteria are capable to, among other resistance mechanisms, secrete β-lactamase enzymes that are capable to inactivate most β-lactam antibiotics by degrading the mentioned four-membered ring.[2]

There are two basic mechanisms for the opening of the β-lactam ring: i) Serine β-lactamases (SBLs),[2] whose catalytic action occurs via acylation-deacylation reactions and ii) Metallo-β-lactamases (MBLs),[3–11] possessing one or two metal (usually Zn^{II}) cations that are capable to hydrolyze the β-lactam ring by deprotonating a coordinated water molecule, which acts as a powerful nucleophile.[12,13] Regarding MBLs, many scientists have devoted their efforts to elucidate their structures as well as catalytic mechanisms,[12,13] aiming at developing efficient inhibitors, which seems to be a titanic effort considering the wide variety of molecular and structural diversity in this family of enzymes.[14,15] In this context, a type of hybrid porous materials, the so-called metal–organic frameworks (MOFs),[16–21] can be helpful to gain information about both structures and catalytic mechanisms of MBLs.

[a] P. Escamilla,[+] Dr. J. Ferrando-Soria, Dr. E. Pardo
Instituto de Ciencia Molecular (ICMOL)
Universitat deValència
Paterna 46980, València (Spain)
E-mail: jesus.ferrando@uv.es
emilio.pardo@uv.es

[b] L. Bartella,[+] R. M. Percoco, Dr. L. Di Donna, M. Prejanò, T. Marino, Dr. D. Armentano
Dipartimento di Chimica e Tecnologie Chimiche
Università della Calabria
87030, Rende, Cosenza (Italy)
E-mail: donatella.armentano@unical.it

[c] L. Bartella,[+] Dr. L. Di Donna
QUASIORA Laboratory, AGRINFRA Research Net
Università della Calabria
87036, Rende, Cosenza (Italy)

[d] S. Sanz-Navarro,[+] Dr. A. Leyva-Pérez
Instituto de Tecnología Química
Universidad Politècnica de València-Consejo Superior de Investigaciones Científicas (UPV-CSIC)
46022 Valencia (Spain)
E-mail: anleyva@itq.upv.ies

[+] These authors contributed equally to this work.

Supporting information for this article is available on the WWW under https://doi.org/10.1002/chem.202301325

MOFs are crystalline porous materials,[22] formed by the combination of metal atoms and organic ligands, exhibiting a seemingly endless diversity of architectures. They have found application, in recent years, in many different important research fields like gas adsorption and separation,[23] transport,[24] water remediation[25] or catalysis.[26,27] More recently, MOFs have become relevant in another emergent field of research as enzymatic catalysis.[28,29] Indeed, several recent publications report MOFs that are capable to carry out, efficiently, enzymatic catalytic reactions.[30–34] The amazing host–guest chemistry[35,36] of MOFs lie at the origin of such efficiency, as they offer the possibility to mimic active sites of enzymes,[30] by a proper combination of metal cations and functional groups within their channels or even encapsulating fragments of small enzymes. For example, we recently reported a metal–organic framework with formula $\{Ca^{II}Cu^{II}_6[(S,S)\text{-serimox}]_3(OH)_2(H_2O)\}\cdot 39H_2O$ (where serimox[36–38] = bis[(*S*)-serine]oxalyl diamide), presenting hexagonal channels densely decorated with methyl alcohol "arms", which exhibited efficient hydrolase-like catalysis.[39]

Herein, we report the preparation of a new highly robust and crystalline Zn_6Ca MOF (Figure 1) -derived from the amino acid *S*-methyl-*L*-cysteine and whose micro-channels are thus decorated with thioether groups- with formula $\{Ca^{II}Zn^{II}_6[(S,S)\text{-Mecysmox}]_3(OH)_2(H_2O)\}\cdot 12H_2O$ (**1**) [Mecysmox = bis[*S*-methyl-L-cysteine]oxalyl diamide], which is capable to accommodate and degrade, very efficiently, amoxicillin and ceftriaxone antibiotics by following two different mechanisms (Figure 2). For amoxicillin, MOF **1** acts as a β-lactamase mimic and expands the very limited number of MOFs capable to mimic catalytic enzymatic processes.[40–42] Remarkably, given the high crystallinity of the Zn_6Ca MOF, single-crystal X-ray diffraction (SCXRD) studies (Table S1) allowed to gain insightful views about the chemical environment of Zn^{II} cations, aiming at further unveiling the mechanisms governing the catalytic action of MBLs. In turn, MOF **1** is also capable to degrade ceftriaxone, but following a different mechanism. Indeed, **1** is capable to efficiently hydrolyze ceftriaxone into thiotriazinone and 3-desacetyl cefotaxime, a reaction that without catalyst only occurs after 12 h. at pH = 5,[43] while leaving unchanged its four-membered β-lactam ring.

Moreover, we have been capable to isolate and characterize, by single-crystal X-ray diffraction (SCXRD), a host guest aggregate containing MOF **1** and amoxicillin (see below, Figure 3), aiming at achieving unique snapshots of the host–guest interactions, ultimately responsible for the β-lactamase activity. The crystal structure of this aggregate allowed us to carry out density functional calculations, which somehow confirm that the hydrolysis of the amoxicillin proceeds through

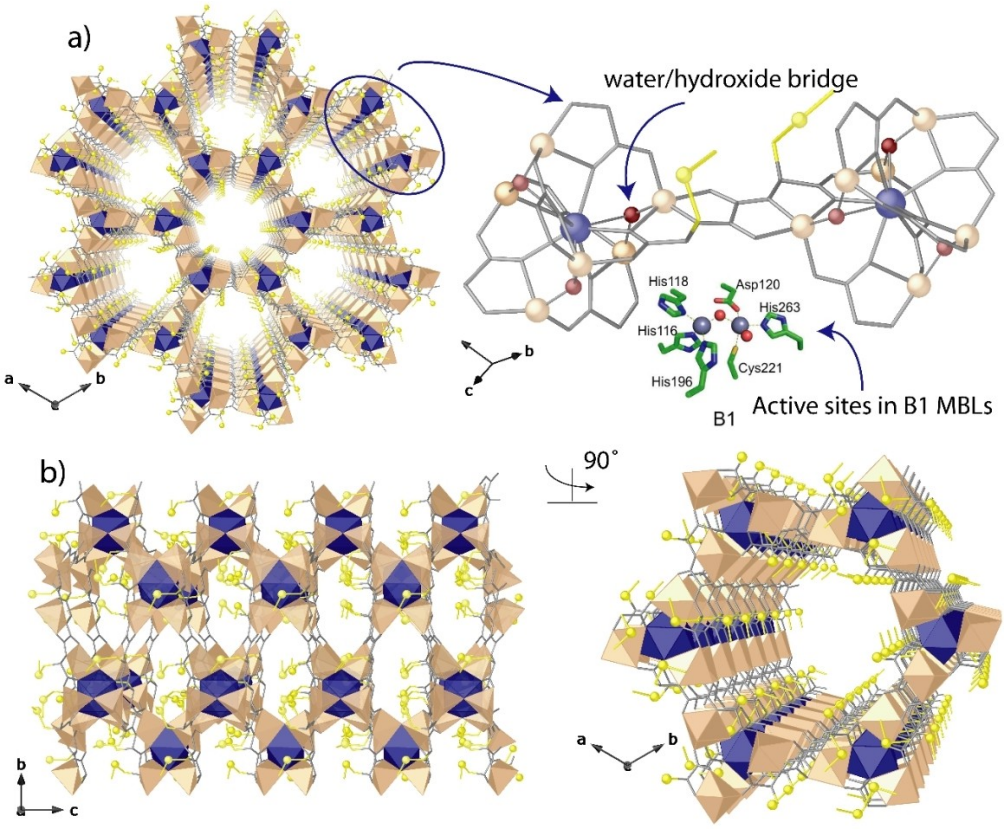

Figure 1. Crystal structure of **1**. a) Perspective views of 3D porous network of **1** along *c* crystallographic axis and a fragment (SBU) of **1** showing the dianionic bis(hydroxo)dizinc(II) building blocks. The inset shows a representative active-site Zn^{II} coordination geometry for B1 enzymes from Metallo-β-lactamases (MBLs), where Zn^{II} ions and water molecules/hydroxide ions are displayed as gray and red spheres, respectively. (b)Views of a fragment of **1** in the *bc* and *ab* planes. Zn, Ca and S atoms are represented by pale orange polyhedra, blue polyhedra, and yellow spheres, respectively, whereas the ligands(except sulfur) are depicted as gray sticks.

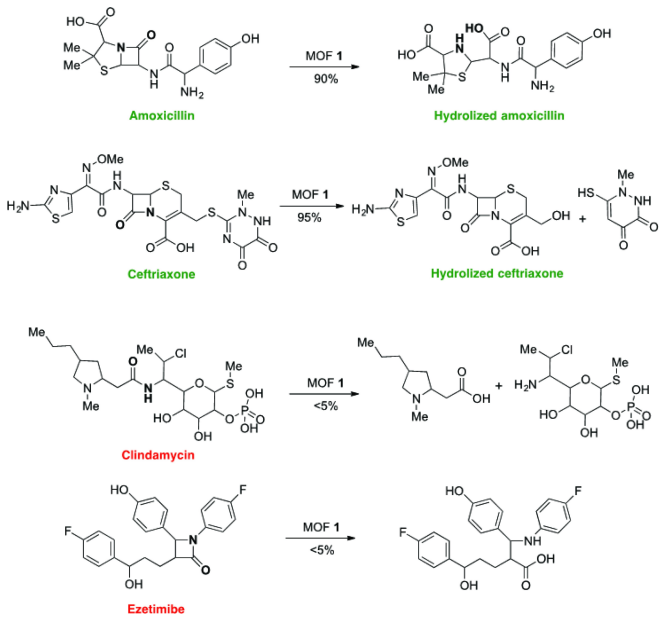

Figure 2. Hydrolysis products of the different antibiotics catalyzed by MOF **1**.

the activation of a water molecule, promoted by Zn-bridging hydroxyl group, concertedly to the nucleophilic attack to the carbonyl moiety and the cleaving of C–N bond of the lactam ring.

Results and Discussion

Synthesis and characterization of MOF 1 and amoxicillin@1

Compound **1** was first synthesized, in a multigram scale, by direct precipitation in water (see experimental section). The resulting polycrystalline powdered sample of **1** was used to carry out analytical/catalytic experiments. Alternatively, compound **1** could be also obtained as colorless hexagonal prisms, using a slow diffusion technique (see experimental section in the Supporting Information). Then, single crystals of **1** were used to determine the crystal structures of the pristine MOF **1** and also a hybrid host–guest aggregate, so-called **amoxicillin@1**, that was obtained after immersing crystals of **1** in saturated DMF solutions of amoxicillin for 72 h.

In addition to the structural characterization (see below), the chemical identity of **1** (and also that of **amoxicillin@1**) was also stablished by elemental analyses (C, H, S, N), inductively coupled plasm-mass spectrometry (ICP-MS), powder X-ray diffraction (PXRD) and thermo-gravimetric (TGA) analyses. Both C, H, S, N analyses and ICP-MS measurements, together with TGA analyses, allowed to determine the chemical formulas of **1** and **amoxicillin@1** (see experimental section). Figures S1 and S2 show the TGA analyses for **1** and **amoxicillin@1**, respectively, which allow to determine the water contents established in the chemical formulas (experimental section). Figures S3 and S4 show the experimental powder X-ray diffraction (PXRD) patterns

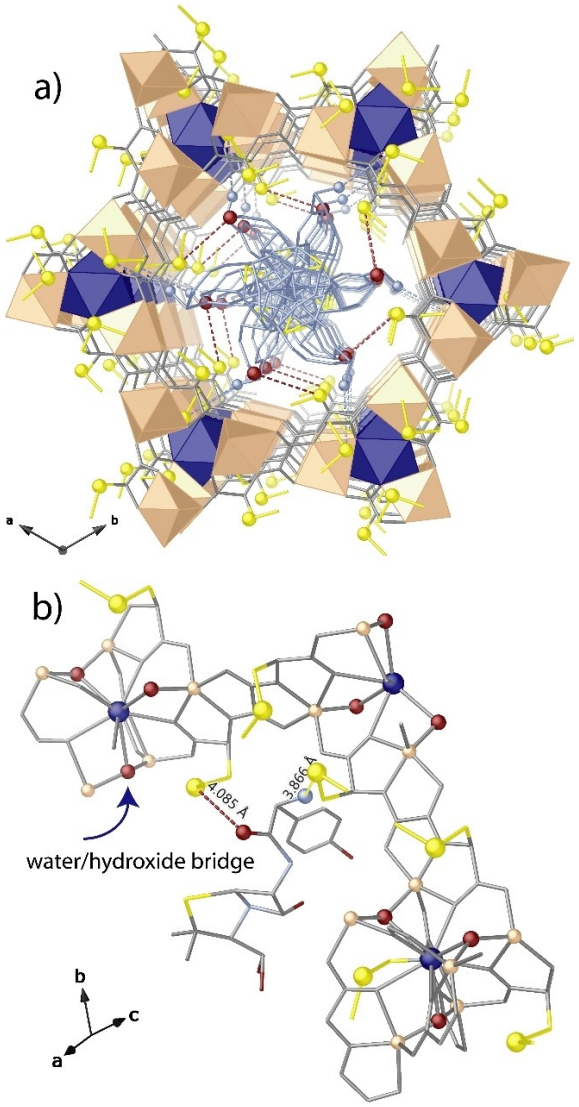

Figure 3. Crystal structure of **amoxicillin@1**. a) Perspective view of a single channel along *c* crystallographic axis. b) Details of host–guest interactions. Zn, Ca and S atoms are represented by pale orange polyhedral (a) or spheres (b), blue polyhedra (a) or spheres (b), and yellow spheres, respectively, whereas the ligands and amoxicillin guest molecules (except nitrogen and oxygen atoms from amoxicillin involved in interactions, sky blue and red spheres, respectively) are depicted as gray, yellow, red and sky blue sticks for carbon, sulfur, nitrogen and oxygen, respectively.

of **1** and **amoxicillin@1**, which are identical to the theoretical ones (Figures S3–S4), confirming the purity and homogeneity of the bulk samples of **1** and **amoxicillin@1**. Finally, aiming at confirming that **1** is capable to host guest antibiotic molecules, its permanent porosity was also evaluated by measuring its N_2 adsorption isotherm (Figure S5). Indeed, the isotherm for **1** shows a type I behavior with large uptake at low pressures. The Brunauer–Emmett–Teller (BET) surface area calculated was 571 m^2/g.[44]

The crystal structure of **1** could be determined by SCXRD (see Supporting Information for structural details). **1** crystallizes in the chiral $P6_3$ space group and consists of chiral honeycomb-like three-dimensional (3D) calcium(II)-zinc(II) networks (Fig-

ure 1) featuring hexagonal channels, of approximately 0.7 nm, where the methylenethiomethyl chains of the amino acid are located (Figures 1b and S6). The 3D porous structure of **1** offers a functional space capable to accommodate/stabilize substrates, in a similar manner to that observed in the active sites in B1 enzymes. The network is constructed from trans-oxamidato-bridged dizinc(II) units, {Zn^{II}_2[(*S*,*S*)-Mecysmox]} (Figure 1a), which act as linkers between the Ca^{II} cations through the carboxylate groups (Figure 1) and are further interconnected, with neighboring dizinc(II) moieties, by water/hydroxide groups (Figure 1a). This situation is reminiscent to that observed in certain MBLs like *S. maltophilia* and *B. fragilis enzimes* (Scheme S1),[45] where hydroxide ions bridge zinc(II) cations. This feature is closely related to metallo-β-lactamases activity, as it is postulated that the catalytic mechanism involves an attack of the metal-bound hydroxide on the carbonyl group of the β-lactam ring, which must be accompanied by the collapse of the four-membered ring.[46]

Indeed, it is well established[45] that Zn^{II} coordination environment is crucial for substrate binding and catalysis in MBLs. Figure 1 shows a detail of the two crystallographically distinct Zn^{II} metal ions in **1**, in similarity with B1 MBLs active sites. B1 enzymes are Zn^{II}-dependent metalloproteins and belong to the Ambler class B enzymes (or metallo-β-lactamases), being one of the three subclasses: B1, B2, and B3.[47] They possess two, Zn1 and Zn2, binding sites containing both a bridging hydroxide and three amino acid residues, but only Zn2 ion is bound to a water molecule (see inset of Figure 1a). As a result, the Zn1 site adopts a tetrahedral coordination geometry (Figure S7), while the Zn2 is trigonal bipyramidal, as both Zn^{II} sites present in MOF **1**. Indeed, in the crystal structure of **1**, Zn^{II} environment is described by a trigonal bipyramidal geometry being coordinated by a nitrogen and three oxygen atoms belonging to the Mecysmox ligand, and a water/hydroxide bridging group (in a 1:2 statistic distribution) as found in B1 enzymes. In the literature there is a general agreement supporting that the active and relevant species of the B1 (and B3) enzymes is the binuclear form.[48] The canonical binuclear site of B1 MBLs exhibit Zn–Zn and Zn–Zn OH distances ranging from 3.5 to 3.9 and 1.9 to 2.2 Å, respectively in the inactive state. In **1**, the Zn-OH bond length is of 1.97(1) Å, with a Zn–Zn distance across the hydroxide bridge of 3.70 Å.

Analytical experiments

On the basis of the structural characteristic observed for the Zn^{II} active sites of the MOF **1**, we carried out analytical experiments to observe if, as we expected, **1** was capable to degrade, selectively, the four-membered rings of amoxicillin and ceftriaxone antibiotics, together with non-penicillinic antibiotics like clindamycin and cholesterol absorption inhibitor ezetimibe, for the sake of comparison (Scheme S2). Notice that ezetimibe also contains a β-lactam ring but not the fused thiazolidine ring. The uptake efficiency of MOF **1** for amoxicillin, ceftriaxone and clindamycin was first evaluated by HPLC-UV analyses in water (see Experimental section for further details).

Regarding amoxicillin degradation, after just 30 min of soaking, the HPLC chromatogram shows the appearance of two UV peaks at rt 6.28 min (**f1**) and 7.12 min (**f2**), in addition to the amoxicillin peak (rt 9.57 min). The area of the first peak (rt 6.28 min) increases as the area relative to amoxicillin peak (9.57 min) decreases, reaching a maximum after 4 h and remaining constant (after 24 h, Figure S8). This evidence suggests the formation of probable degradation products of amoxicillin. The fractions **f1** and **f2** collected from HPLC separation were, hence, analyzed by mass spectrometry in order to retrieve structural information. The HPLC-MS determination was performed at high resolution using an Orbitrap Exploris 120 equipped with an ESI source. The full MS spectra of both fractions carried out in positive mode showed similar protonated molecular ions at m/z 384.1224 which matches with the formula $C_{16}H_{22}N_3O_6S$. The elemental composition corresponds to the amoxicillin penicilloic acid compound (Figure S9). The presence of the same m/z signal at different retention times may be rationalized by the formation in solution of two epimers, as already reported in literature.[49] Furthermore, the HR-MS analysis showed the presence of the two epimers of amoxicillin penicilloic acid compounds (m/z 340.1311), derived from a consecutive decarboxylation of amoxicillin penicilloic acid (m/z 384.1224). This decarboxylation probably occurs in solution and it is not affected by MOF. The presence of stereoisomers was confirmed by MS/MS experiments, which disclose the same fragmentation pattern (Figure S10).

In order to support the ring opening reaction mechanism, the soaking was performed also in MeOH. After 24 h the HPLC-ESI MS analysis showed the presence of just one peak relative to the formation of the methyl ester of the amoxicillin penicilloic acid (Figure S11). In this case, as expected, no decarboxylation product was detected, and no epimerization occurred.[50]

The situation is drastically different for the cephalosporin β-lactam antibiotic ceftriaxone. Indeed, a different hydrolysis reaction mechanism is observed when ceftriaxone is soaked with MOF **1**. The HPLC-UV analysis shows, as a matter of fact, the formation of only one degradation product (Figure S12), which has been identified by HPLC-ESI-HRMS as the ion at m/z 414.0535 (Figure S13). This compound is produced by the hydrolysis of ceftriaxone at the sulfur atom of the carbamimidothioate group, previously characterized after hydrolysis at pH = 5 after 12 days.[43]

Finally, clindamycin, which belongs to the class of lincosamide antibiotics, does not show any hydrolytic behavior when soaked with MOF **1**. Furthermore, the uptake of the molecule reaches a maximum at 5 h, and then decreases at the initial level, showing a behavior governed almost completely by physisorption mechanisms.

Catalytic experiments

Aiming at further confirming the degrading activity of MOF **1** towards amoxicillin and ceftriaxone, we also carried out catalytic experiments. Reactions were followed by in-situ by

proton nuclear magnetic resonance (^{1}H NMR), diffuse reflectance ultraviolet-visible spectrophotometry (DR-UV-vis) and Fourier transformed infrared spectroscopy (FTIR). A parent MOF, non-containing Zn but Cu, with formula ({$Ca^{II}Cu^{II}_6$[(*S,S*)-Mecysmox]$_3$(OH)$_2$(H_2O)}·16H_2O (MOF **2**))[51,52] and also ZnO were evaluated as catalysts for the same reaction. The results are shown in Table 1 and Figure 2.

^{1}H NMR results (Figure S14) show that MOF **1**, containing Zn^{II} sites, catalyzes very efficiently and selectively (90% yield) the hydrolysis of the β-lactam ring in amoxicillin, keeping untouched the rest of bonds in the molecules, which include, among others, linear amide, oxime, thioamines and diazine bonds. The same efficiency (>90% yield) is observed for the degradation of ceftriaxone to give into thiotriazinone and 3-desacetyl cefotaxime (Figure S15). DR-UV-vis (Figure S16) and FTIR (Figure S17) measurements confirm the presence of the hydrolyzed products inside the framework of MOF **1** after reaction. In accordance, the linear amide bond of the non-penicillinic antibiotic clindamycin does not react under identical reaction conditions (Figure S18), and even the β-lactam ring of the cholesterol absorption inhibitor ezetimibe is completely unreactive (Figure S19), which supports the high selectivity of MOF **1** towards the fused β-lactam-thiazolidine ring core and discards an enhanced amide hydrolysis reaction by pure confinement effects.[53] MOF **2**, containing Cu^{II} cations in its framework instead of Zn^{II} ones, is completely inactive towards the hydrolysis reaction, confirming that neither Cu^{II} cations nor Ca^{II} ones play a relevant role in the degradation reaction. In turn, ZnO shows some catalytic activity, but much lower than MOF **1**. These results, together, support the uniqueness of the Zn^{II} sites in MOF **1** to catalyze the hydrolysis of the β-lactam ring in penicillinic antibiotics, such as β-lactamases do, and the potential role of simple MOFs as biocatalysts.[54] Finally, ICP-MS analyses (see experimental section in the Supporting Information) and PXRD (Figure S20) measurements for MOF **1**, after the catalytic study, confirm that the chemical formula remains unaltered and that no degradation of the MOF is observed during the catalytic experiments.

Table 1. Catalytic results for the hydrolysis reaction of different penicillinic and non-penicillinic antibiotics in the presence of different solids. 20 mol% Zn.

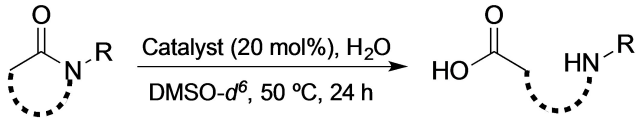

Entry	Substrate	Catalyst	Conversion [%][a]
1	Amoxicillin	MOF **1**	90
2		MOF **2**	<5
3		ZnO	60
4	Ceftriaxone	MOF **1**	95
5		MOF **2**	<5
6		ZnO	50
7	Clindamycin and ezetimibe	MOF **1**	<5
8		MOF **2**	<5
9		ZnO	<5

[a] Conversions measured by ^{1}H NMR spectroscopy.

The crystal structure of the host–guest aggregate **amoxicillin@1** helps to gain further information about the nature of the host–guest interaction as well as the concomitant β-lactamase activity. Aiming at acquiring structural insights, we soaked crystals of **1** within water, methanol and dimethylformamide saturated solutions containing amoxicillin (details in Experimental Section and Supporting Information). Only DMF solution allowed to observe a single-crystal-to-single-crystal process of amoxicillin insertion, further supporting the proposed catalytic reaction mechanism. Indeed, in water and methanol, after 24 h the HPLC-ESI(+)-Orbitrap MS analysis detected the formation of amoxicillin penicilloic acid and its methyl ester, respectively (Figures S9 and S11). with the consequent loss of crystallinity of **1**, likely related to the required rearrangement of Zn^{II} metal nodes during the catalytic reaction. After the encapsulation in DMF, we have obtained amoxicillin@{$Ca^{II}Zn^{II}_6$[(*S,S*)-Mecysmox]$_3$(OH)$_2$(H_2O)}·9H_2O (**amoxicillin@1**) adsorbate. The retained crystallinity of the **amoxicillin@1** adsorbate allowed the use of SCXRD to determine its crystal structure. This allows visualizing the robustness of **1**, the accomplished molecules captured and the structural stability of the final adsorbate. Although the guest molecules were highly disordered in the pores (Supporting Information for refinement details), we succeeded in obtaining their most probable locations and even their interaction sites with MOF **1** hosting matrix (Figures 3 and S21–S22).

Amoxicillin@1 is isomorphic to **1**, crystallizing in the $P6_3$ chiral space group of the hexagonal system. This structural feature confirms the robustness of the 3D network of **1**, even after antibiotic encapsulation. In the crystal structure, amoxicillin guest molecules are confined in the hexagonal pores of **1**, being recognized by the sulfur atoms of the *S*-methyl-*L*-cysteine residues (Figure 3). They are stabilized by σ-hole interactions[55] involving nitrogen and oxygen atoms of the target molecules with the amino acid moieties. As expected, after process of encapsulation in MOFs, amoxicillin molecules show statistical and thermal disorder. In fact, it was not possible to found from ΔF maps the terminal methyl and carboxylic fragments of the guest molecules (Figure S22), because an overlapping with equivalent detected carbon and nitrogen atoms occurs (see Crystallographic Supporting Information for details). The evidence of σ-hole interactions is given by -CH_2SCH_3 *S*-methyl-*L*-cysteine arms pointing toward the -NH_2 group [S···N distance of 3.87(1) Å] and the internal carbonyl groups atoms [S···O distance of 4.09(1) Å] of the amoxicillin (Figure 3b). These interactions represent an intrinsic feature of this sulfur containing MOFs, for which non-covalent contacts can be ensured via the low-lying σ* orbitals of the C–S bond (σ-hole), available for interaction with electron donors.[55] As previously anticipated, the active site of MBLs resides sandwiched between two β-sheets that represent the borders of the two halves of the protein (Figure 1a, inset). The general shared mechanism of the active site proposes one or two zinc ions, responsible for substrate binding and catalysis, located in these particular positions by ligands' coordination. In similarity with this picture, in pores of **1**, substrate molecules, thanks to the clutching action of sulfur atoms from the *S*-methyl-*L*-cysteine moieties, and water-medi-

ated host–guest hydrogen bonds ensured by lattice waters in confined space and nucleophilic hydroxide/water bridge, easily approach one of the two Zn trigonal bipyramidal positions in each Zn-$(OH)_2(H_2O)$-Zn dimeric entity. In so doing, one of the two activated Zn sites acts in substrate binding by coordinating one of the carboxylate present in the non-β-lactam ring of the antibiotic and likely stabilizing an anionic intermediate. In this scenario, the nucleophilic hydroxide/water remains coordinated only to the second activated Zn site. This second step is not observed in DMF, where water-mediated non-covalent interactions are not provided, as shown in **amoxicillin@1** crystal structure and explain the loss of crystallinity of **1** in H_2O and MeOH, related to the required metal nodes environment rearrangement.

Overall, crystal structure of **amoxicillin@1** permits to unveil certain aspects of the mechanism governing the β-lactamase activity of MOF **1**. It relies in a proper immobilization of the guest molecule, by the properly designed thioether groups within MOF channels, and the concomitant hydrolysis by the water positioned by one of the two metal binding sites water/hydroxo bridged, which show an essential and functional role.

Theoretical calculations

To further confirm the β-lactamase activity of MOF **1**, Density Functional Theory (DFT) calculations were carried out on a model (Table S2) of **amoxicillin@1** system as depicted in Figures 4a, S23 and S24. The model was built up following the quantum-chemical cluster approach scheme, which was successfully applied on a number of similar chemical systems[56,57] (see Supporting Information). The technical details are fully described in the Supporting Information. Two water mediated reaction mechanisms were investigated for the hydrolysis of the amoxicillin (see Figure 4b). In mechanism **A**, the Zn-bridging hydroxyl group activates the water molecule, by accepting one proton, and the formed nucleophilic species ($O_{w1}H^-$) is able to attack the β-lactam carbonyl group of the substrate, causing the opening of the four-membered ring. In the alternative **B** mechanism, the nucleophilic attack to the carbonyl group takes place directly by the O_{w1} with the consequent cleavage of C–N bond. The final product, for both considered mechanisms, is characterized by the formed carboxylic and NH- groups originating from the opening of the ring (Figure 4b). The analysis of the energy barriers reveals a more energetic feasibility of the mechanism **A**, since **TSB** lies at 9.5 kcal/mol higher than the **TSA** (23.9 kcal/mol vs 14.4 kcal/mol, see Figure 4b). Despite both calculated barriers are not prohibitive for the catalysis, in mechanism **A** is evident the role played by the Zn^{II} centers, which boost the reaction promoting the formation of a good nucleophile. The driving force of the reaction is the concerted formation of C–C and breaking of C–N bonds, further confirmed by the imaginary frequency of 376.1*i* cm^{-1}, and the formation of NH group, which occurs spontaneously due to the hydrogen-bond network involving the w1, w2 and the scaffold of the MOF **1** (see Figure 4c). The ordered composition of MOF **1** is therefore the origin of the catalytic action, leading to the occurrence of the reaction with reason-

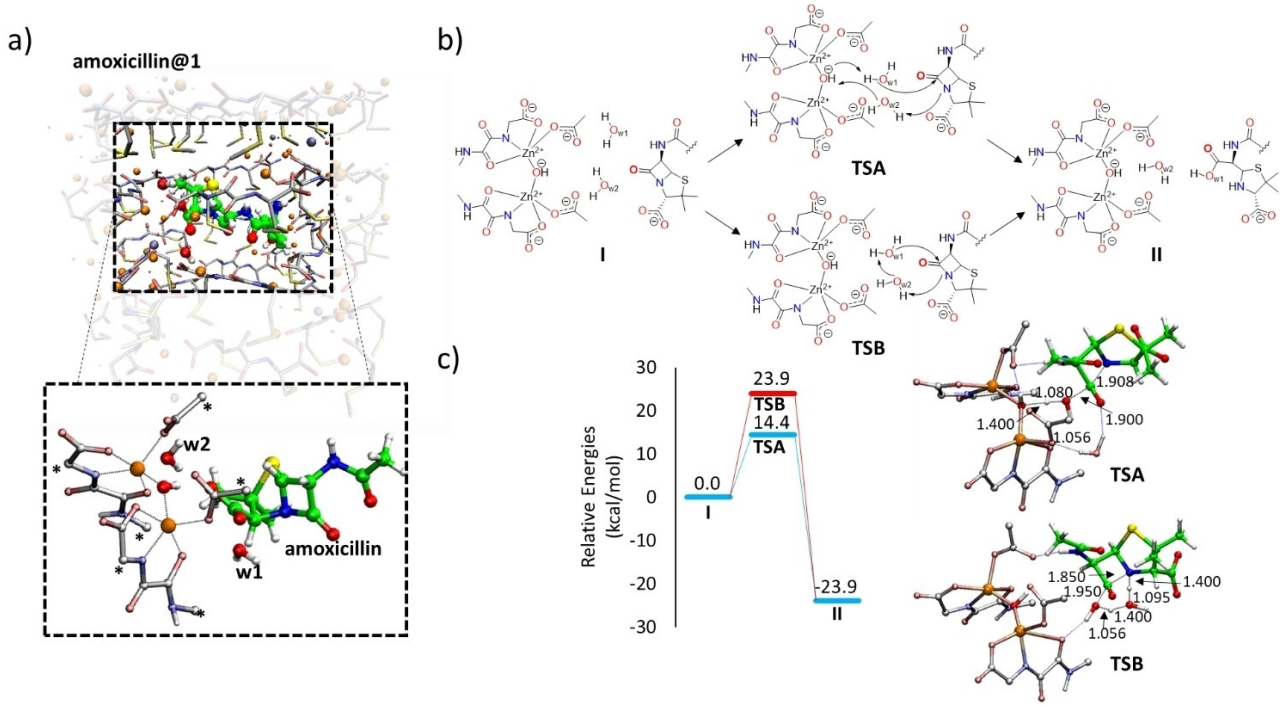

Figure 4. DFT study of amoxicillin hydrolysis by MOF **1**. a) The adopted model where the atoms labelled with "*" were kept fixed in their crystal coordinates. b) The investigated water-mediated mechanisms, c) the related calculated energy profiles and the optimized geometries of transition states (distances in Å). In a) and c) Zn, O, S, N and H were represented by orange, red, yellow, blue and white spheres, respectively, while C atoms of amoxicillin were represented as green spheres (in silver the others). For clarity, most of the non-polar hydrogens were omitted in the representation.

able kinetic, in addition to the favorable thermodynamics (−23.9 kcal/mol). The proposed mechanism, and the here-described role of the Zn^{II} ions, invokes the working mechanism proposed for β-lactamases.[7,8,12] Furthermore, the calculated energy barrier for **TSA** (14.4 kcal/mol) is in good agreement with the available kinetic data, concerning the action of the enzyme from different microorganisms on amoxicillin, as evidenced by turnover numbers from 2 s^{-1} to 910 s^{-1}.[58,59] These values converted in activation energies correspond to barriers in the range of 13 to 17 kcal/mol, which are close to the calculated one.

Conclusions

In summary, we report a novel 3D Zn-based MOF (**1**), derived from amino acid *S*-methyl-*L*-cysteine, possessing functional channels, densely decorated with thioether functional groups, which are capable to immobilize, amoxicillin and ceftriaxone antibiotics by means of efficient host–guest interactions. Then, in a second step, **1** catalyzes the selective hydrolysis of these β-Lactam antibiotics. For ceftriaxone, **1** induces its hydrolysis into thiotriazinone and 3-desacetyl cefotaxime, a reaction that usually only occurs without the catalyst at pH = 5. On the other hand, **1** degrades, very efficiently, the four-membered β-lactam ring of amoxicillin, acting as a β-lactamase mimic and expands the very limited number of MOFs capable to mimic catalytic enzymatic processes. Single-crystal X-ray diffraction studies allowed to resolve the crystal structure of the host–guest aggregate **amoxicillin@1**, which permits to gain unique snap-shots on the host guest-interactions between the functional channels of the MOF and amoxicillin, responsible for the guest encapsulation/retention, as well as on the Zn^{II} coordination environment responsible for the enzymatic catalysis. On the basis of this crystallographic data, a plausible mechanism for this β-lactamase activity has been proposed by means of DFT calculations, which is a clear step forward on the understanding of β-lactamase enzymes.

Experimental Section

Preparation of $\{Zn_6Ca[(S,S)\text{-Mecysmox}]_3(OH)_2(H_2O)\}\cdot 12H_2O$ (1): An aqueous solution (35 mL) of H_2Me_2-(*S,S*)-Mecysmox (2.1 g, 6 mmol) and a 25% methanolic solution of Me_4NOH (7.25 mL, 18 mmol) were added dropwise to another aqueous solution of $Zn(NO_3)_2\cdot 6H_2O$ (3.55 g, 12 mmol) and $CaCl_2$ (0.22 g, 2 mmol) in 20 mL. The solution mixture was stirred overnight and a white powder was obtained and collected by filtration, washed with water and methanol. Yield: 1.87 g, 56%. Anal.: calcd. for $C_{30}H_{64}N_6O_{33}S_6Zn_6Ca$ (1661.7): C, 21.68; H, 3.88; N, 5.06; S, 11.58%. Found: C, 21.67; H, 3.72; N, 5.06; S, 11.47%. IR (KBr): ν = 1603 cm^{-1} (C=O).

Suitable single crystals of **1** for X-ray structural analysis were obtained by slow diffusion, in an H-shaped tube, of H_2O/DMF (1:1) solutions containing stoichiometric amounts of H_2Me_2-(*S,S*)-Mecysmox (0.064 g, 0.18 mmol) and a 25% aqueous solution of Me_4NOH (0.22 mL, 0.54 mmol) in one arm and $Zn(NO_3)_2\cdot 6H_2O$ (0.11 g, 0.36 mmol) and $CaCl_2$ (0.007 g, 0.06 mmol) in the other. They were isolated by filtration on paper and air-dried. Anal.: calcd. for $C_{30}H_{64}N_6O_{33}S_6Zn_6Ca$ (1661.7): C, 21.68; H, 3.88; N, 5.06; S, 11.58%. Found: C, 21.71; H, 3.93; N, 4.99; S, 11.67%. IR (KBr): ν = 1601 cm^{-1} (C=O). After catalytic experiments, elemental C, H, S, N and ICP-MS analyses confirmed that the chemical formula remained unaltered with the only exception of several crystallization water molecules. These analyses have been included in the following chemical formula: $C_{30}H_{46}N_6O_{24}S_6Zn_6Ca$ (1499.5). Anal.: calcd.: C, 24.03; H, 3.09; N, 5.60; S, 12.83%. Found: C, 24.13; H, 2.99; N, 5.719; S, 12.79%.

Preparation of $(C_{16}H_{19}N_3O_5S)@\{Zn^{II}Cu^{II}_6[(S,S)\text{-Mecysmox}]_3(OH)_2(H_2O)\}\cdot 9H_2O$ (amoxicillin@1): Well-formed hexagonal green prisms of **amoxicillin@1**, which were suitable for X-ray diffraction, were obtained by soaking crystals of **1** (5.0 mg) in a saturated dimethylformamide solution of amoxicillin for 72 h. The crystals were washed with water, isolated by filtration on paper and air-dried. Anal.: calcd for $C_{46}Zn_6CaH_{77}S_7N_9O_{35}$ (1973.0): C, 28.00; H, 3.93; S, 11.38; N, 6.39%. Found: C, 28.07; H, 3.81; S, 11.29; N, 6.41%. IR (KBr): ν = 1603 cm^{-1} (C=O).

Analytical experiments: The uptake measurements for amoxicillin and ceftriaxone were performed by using a HPLC-UV instrument (Water FractionLynx System). The chromatographic separations were carried out employing a reverse-phase Luna C_{18} (2) column (250×4.6 mm; Phenomenex, Torrance, CA). An isocratic elution with 0.1% formic acid and methanol (96:4 v/v) was used for the amoxicillin determination, while an isocratic elution with 0.1% formic acid in water and acetonitrile (85:15 v/v) was used for the determination of Ceftriaxone. The run time was 15 min, whereas the flow rate and the UV wavelength were set to 1.5 and 230 nm for amoxicillin and 1.0 mL/min and 242 nm for ceftriaxone. The injection volume was 20 μL. The calibration curve was obtained by injecting the standard solutions in the range of concentration from 25 to 400 mg/L. The chromatograms have been collected after 30 min, 4 h and 24 h of soaking.

Catalysis details: All reactions were performed under aerobic solvent-free conditions. The corresponding amount of MOF 1 (typically 18 mg, 20 mol% Zn) and DMSO-d^6 (typically 0.8 mL) were placed in a 2 mL vial equipped with a magnetic stir bar. Then, the corresponding compound (e.g., 20 mg, 0.05 mmol for amoxicillin) was added at room temperature. The mixture was sealed and magnetically stirred in a pre-heated steel block at 50 °C for 24 h. After that time, the reaction mixture was passed through a 25 μm filter syringe and submitted to NMR analysis.

X-ray powder diffraction measurements: Polycrystalline samples of **1** and **amoxicillin@1** were introduced into 0.5 mm borosilicate capillaries prior to being mounted and aligned on a Empyrean PANalytical powder diffractometer, using Cu Kα radiation (λ = 1.54056 Å). For each sample, five repeated measurements were collected at room temperature (2θ = 2–60°) and merged in a single diffractogram.

X-ray crystallographic data collection and structure refinement: Crystals of **1** and **amoxicillin@1** were selected and mounted on a MITIGEN holder in paratone oil. Diffraction data were collected on a Bruker-Nonius X8APEXII CCD area detector diffractometer, at 100 K (**1**) and room temperature (**amoxicillin@1**), using graphite-monochromated Mo–Kα radiation (λ = 0.71073 Å). See Supporting Information for further details. Deposition Number(s) 2258088 (for **1**) and 2258089 (for **amoxicillin@1**) contain(s) the supplementary crystallographic data for this paper. These data are provided free of charge by the joint Cambridge Crystallographic Data Centre and Fachinformationszentrum Karlsruhe Access Structures service.

Computational details: The amoxicillin substrate has been docked in a section of the MOF **1**, representing the minimal unit of the crystal (23.74×27.45×19.50 $Å^3$). For the molecular recognition, AutoDock Vina software[66] has been adopted and nine output

structures of amoxicillin binding **1** have been generated. To investigate complete pore's conformational space, the box centroid has been set by geometric center of the model (coordinates x,y,z = −0.346, 0.068, 0.809), selecting 40 for X,Y and 60 for Z as parameters for the grid point generation. The obtained docked conformations of amoxicillin have been analyzed and the best one (lowest binding affinity, see Table S2) has been selected for later quantum chemical investigation. In the lowest binding mode, the substrate engages σ-hole interactions with the -SCH_3 groups of MOF scaffold, similarly to the observations arising from the crystal structure analysis (see Figure S22). The carbonyl of the amide bond indeed lies at 4.77 Å from one of thio-methyl moiety while the amino group is at 4.03 Å from another one (4.09 Å and 3.87 Å in the crystal structure, respectively). See Supporting Information for further details.

Supporting Information

Analytical, catalytic, crystallographic and theoretical calculations details, PXRD, adsorption isotherms, HPLC, NMR, UV-vis, FTIR and TGA data. Additional references cited within the Supporting Information.[51,60–73]

Acknowledgements

This work was supported by the MICINN (Spain) (Projects PID2019-104778GB-I00, PID2020-115100GB-I00, and Excellence Units "Severo Ochoa" CEX2021-001230-S and "Maria de Maeztu" CEX2019-000919-M) and the Ministero dell'Istruzione, dell'Università e della Ricerca (Italy). The work has also been funded by Generalitat Valenciana, Prometeo Grupos de Investigación de Excelencia (PROMETEU/2021/054). D.A. also acknowledges the financial support of the European Union - NextGenerationEU under the National Recovery and Resilience Plan (NRRP) of Ministero dell'Università e della Ricerca (MUR) (Project code PE0000021, "Network 4 Energy Sustainable Transition - NEST). Thanks are also extended to the 2019 Post-doctoral Junior Leader-Retaining Fellowship, la Caixa Foundation (ID100010434 and fellowship code LCF/BQ/PR19/11700011), the "Generalitat Valenciana" (SEJI/2020/034) and the "Ramón y Cajal" program (J.F.-S.). E.P. acknowledges the financial support of the European Research Council under the European Union's Horizon 2020 research and innovation programme / ERC Grant Agreement No 814804, MOF-reactors. S.S.-N. thanks a fellowship from MINECO (project number CTQ 2017–86735-P). This study forms part of the Advanced Materials programme (MFA/2022/048) and was supported by MCIN with funding from European Union NextGenerationEU (PRTR-C17.I1) and by Generalitat Valenciana. Financial support from Dipartimento di Chimica e Tecnologie Chimiche (CTC), Università della Calabria, is also gratefully acknowledged for computational investigation.

Conflict of Interests

The authors declare no competing interests.

Data Availability Statement

The data that support the findings of this study are available in the Supporting Information of this article and from the corresponding author upon reasonable request.

Keywords: biomimicry · β-lactamase · enzymatic catalysis · metal–organic framework · zinc

[1] S. A. Testero, L. I. Llarrull, J. F. Fisher, S. Mobashery, in *Burger's Med. Chem. Drug Discov.*, Wiley, **2021**, pp. 1–188.
[2] C. L. Tooke, P. Hinchliffe, E. C. Bragginton, C. K. Colenso, V. H. A. Hirvonen, Y. Takebayashi, J. Spencer, *J. Mol. Biol.* **2019**, *431*, 3472–3500.
[3] N. V. Kaminskaia, B. Spingler, S. J. Lippard, *J. Am. Chem. Soc.* **2000**, *122*, 6411–6422.
[4] A. Tamilselvi, M. Nethaji, G. Mugesh, *Chem. Eur. J.* **2006**, *12*, 7797–7806.
[5] A. Tamilselvi, G. Mugesh, *JBIC J. Biol. Inorg. Chem.* **2008**, *13*, 1039–1053.
[6] A. D. Naik, J. Beck, M. M. Dîrtu, C. Bebrone, B. Tinant, K. Robeyns, J. Marchand-Brynaert, Y. Garcia, *Inorganica Chim. Acta* **2011**, *368*, 21–28.
[7] M. Umayal, G. Mugesh, *Inorganica Chim. Acta* **2011**, *372*, 353–361.
[8] A. Tamilselvi, G. Mugesh, *Inorg. Chem.* **2011**, *50*, 749–756.
[9] L. J. Daumann, L. R. Gahan, P. Comba, G. Schenk, *Inorg. Chem.* **2012**, *51*, 7669–7681.
[10] S. Wöckel, J. Galezowska, S. Dechert, F. Meyer, *Inorg. Chem.* **2012**, *51*, 2486–2493.
[11] L. J. Daumann, G. Schenk, L. R. Gahan, *Eur. J. Inorg. Chem.* **2014**, *2014*, 2869–2885.
[12] J. H. Ullah, T. R. Walsh, I. A. Taylor, D. C. Emery, C. S. Verma, S. J. Gamblin, J. Spencer, *J. Mol. Biol.* **1998**, *284*, 125–136.
[13] G. Garau, C. Bebrone, C. Anne, M. Galleni, J.-M. Frère, O. Dideberg, *J. Mol. Biol.* **2005**, *345*, 785–795.
[14] M. Galleni, J. Lamotte-Brasseur, G. M. Rossolini, J. Spencer, O. Dideberg, J.-M. Frère, *Antimicrob. Agents Chemother.* **2001**, *45*, 660–663.
[15] P. E. Tomatis, R. M. Rasia, L. Segovia, A. J. Vila, *Proc. Natl. Acad. Sci.* **2005**, *102*, 13761–13766.
[16] H. Furukawa, K. E. Cordova, M. O'Keeffe, O. M. Yaghi, *Science* **2013**, *341*, 974.
[17] H.-C. Zhou, S. Kitagawa, *Chem. Soc. Rev.* **2014**, *43*, 5415–5418.
[18] Y. Cui, B. Li, H. He, W. Zhou, B. Chen, G. Qian, *Acc. Chem. Res.* **2016**, *49*, 483–493.
[19] G. Maurin, C. Serre, A. Cooper, G. Férey, *Chem. Soc. Rev.* **2017**, *46*, 3104–3107.
[20] T. He, X.-J. Kong, J.-R. Li, *Acc. Chem. Res.* **2021**, *54*, 3083–3094.
[21] R. Freund, O. Zaremba, G. Arnauts, R. Ameloot, G. Skorupskii, M. Dincă, A. Bavykina, J. Gascon, A. Ejsmont, J. Goscianska, et al., *Angew. Chem. Int. Ed.* **2021**, *60*, 23975–24001.
[22] W. M. Bloch, N. R. Champness, C. J. Doonan, *Angew. Chem. Int. Ed.* **2015**, *54*, 12860–12867.
[23] R.-B. Lin, S. Xiang, W. Zhou, B. Chen, *Chem* **2020**, *6*, 337–363.
[24] L. S. Xie, G. Skorupskii, M. Dincă, *Chem. Rev.* **2020**, *120*, 8536–8580.
[25] M. Mon, R. Bruno, J. Ferrando-Soria, D. Armentano, E. Pardo, *J. Mater. Chem. A* **2018**, *6*, 4912–4947.
[26] D. Yang, B. C. Gates, *ACS Catal.* **2019**, *9*, 1779–1798.
[27] A. Bavykina, N. Kolobov, I. S. Khan, J. A. Bau, A. Ramirez, J. Gascon, *Chem. Rev.* **2020**, *120*, 8468–8535.
[28] Y. Okamoto, T. R. Ward, in *Compr. Supramol. Chem. II*, Elsevier, **2017**, pp. 459–510.
[29] W. Liang, H. Xu, F. Carraro, N. K. Maddigan, Q. Li, S. G. Bell, D. M. Huang, A. Tarzia, M. B. Solomon, H. Amenitsch, et al., *J. Am. Chem. Soc.* **2019**, *141*, 2348–2355.
[30] K. Chen, C.-D. Wu, *Coord. Chem. Rev.* **2019**, *378*, 445–465.
[31] J.-S. Qin, S. Yuan, C. Lollar, J. Pang, A. Alsalme, H.-C. Zhou, *Chem. Commun.* **2018**, *54*, 4231–4249.
[32] X. Lian, Y. Fang, E. Joseph, Q. Wang, J. Li, S. Banerjee, C. Lollar, X. Wang, H.-C. Zhou, *Chem. Soc. Rev.* **2017**, *46*, 3386–3401.
[33] E. Gkaniatsou, C. Sicard, R. Ricoux, J.-P. Mahy, N. Steunou, C. Serre, *Mater. Horizons* **2017**, *4*, 55–63.
[34] I. Nath, J. Chakraborty, F. Verpoort, *Chem. Soc. Rev.* **2016**, *45*, 4127–4170.
[35] M. Kondo, T. Yoshitomi, H. Matsuzaka, S. Kitagawa, K. Seki, *Angew. Chem. Int. Ed. English* **1997**, *36*, 1725–1727.

[36] M. Mon, R. Bruno, J. Ferrando-Soria, L. Bartella, L. Di Donna, M. Talia, R. Lappano, M. Maggiolini, D. Armentano, E. Pardo, *Mater. Horizons* **2018**, *5*, 683–690.
[37] M. Mon, R. Bruno, R. Elliani, A. Tagarelli, X. Qu, S. Chen, J. Ferrando-Soria, D. Armentano, E. Pardo, *Inorg. Chem.* **2018**, *57*, 13895–13900.
[38] M. Mon, R. Bruno, E. Tiburcio, P.-E. Casteran, J. Ferrando-Soria, D. Armentano, E. Pardo, *Chem. Eur. J.* **2018**, *24*, 17712–17718.
[39] M. Mon, R. Bruno, S. Sanz-Navarro, C. Negro, J. Ferrando-Soria, L. Bartella, L. Di Donna, M. Prejanò, T. Marino, A. Leyva-Pérez, et al., *Nat. Commun.* **2020**, *11*, 3080.
[40] A. M. Wright, Z. Wu, G. Zhang, J. L. Mancuso, R. J. Comito, R. W. Day, C. H. Hendon, J. T. Miller, M. Dincă, *Chem* **2018**, *4*, 2894–2901.
[41] D. Feng, Z.-Y. Gu, J.-R. Li, H.-L. Jiang, Z. Wei, H.-C. Zhou, *Angew. Chem. Int. Ed.* **2012**, *51*, 10307–10310.
[42] S. Yuan, L. Zou, H. Li, Y.-P. Chen, J. Qin, Q. Zhang, W. Lu, M. B. Hall, H.-C. Zhou, *Angew. Chem. Int. Ed.* **2016**, *55*, 10776–10780.
[43] A. R. Klein, E. Sarri, S. E. Kelch, J. J. Basinski, S. Vaidya, L. Aristilde, *ACS Earth Sp. Chem.* **2021**, *5*, 1511–1524.
[44] J. Rouquerolt, D. Avnir, C. W. Fairbridge, D. H. Everett, J. H. Haynes, N. Pernicone, J. D. F. Ramsay, K. S. W. Sing, K. K. Unger, *Pure Appl. Chem.* **1994**, *66*, 1739–1758.
[45] G. Bahr, L. J. González, A. J. Vila, *Chem. Rev.* **2021**, *121*, 7957–8094.
[46] N. O. Concha, B. A. Rasmussen, K. Bush, O. Herzberg, *Structure* **1996**, *4*, 823–836.
[47] T. Naas, S. Oueslati, R. A. Bonnin, M. L. Dabos, A. Zavala, L. Dortet, P. Retailleau, B. I. Iorga, *J. Enzyme Inhib. Med. Chem.* **2017**, *32*, 917–919.
[48] J. M. González, M.-R. Meini, P. E. Tomatis, F. J. M. Martín, J. A. Cricco, A. J. Vila, *Nat. Chem. Biol.* **2012**, *8*, 698–700.
[49] I. Gozlan, A. Rotstein, D. Avisar, *Chemosphere* **2013**, *91*, 985–992.
[50] A. A. Taubinger, D. Fenske, J. Podlech, *Tetrahedron* **2008**, *64*, 8659–8667.
[51] R. Bruno, M. Mon, P. Escamilla, J. Ferrando-Soria, E. Esposito, A. Fuoco, M. Monteleone, J. C. Jansen, R. Elliani, A. Tagarelli, et al., *Adv. Funct. Mater.* **2021**, *31*, 2008499.
[52] E. Tiburcio, R. Greco, M. Mon, J. Ballesteros-Soberanas, J. Ferrando-Soria, M. López-Haro, J. C. Hernández-Garrido, J. Oliver-Meseguer, C. Marini, M. Boronat, et al., *J. Am. Chem. Soc.* **2021**, *143*, 2581–2592.
[53] H. Takezawa, K. Shitozawa, M. Fujita, *Nat. Chem.* **2020**, *12*, 574–578.
[54] T.-H. Wei, S.-H. Wu, Y.-D. Huang, W.-S. Lo, B. P. Williams, S.-Y. Chen, H.-C. Yang, Y.-S. Hsu, Z.-Y. Lin, X.-H. Chen, et al., *Nat. Commun.* **2019**, *10*, 5002.
[55] C. Negro, P. Escamilla, R. Bruno, J. Ferrando-Soria, D. Armentano, E. Pardo, *Chem. Eur. J.* **2022**, *28*, e202200034.
[56] M. R. A. Blomberg, T. Borowski, F. Himo, R.-Z. Liao, P. E. M. Siegbahn, *Chem. Rev.* **2014**, *114*, 3601–3658.
[57] M. Prejanò, M. E. Alberto, N. Russo, M. Toscano, T. Marino, *Catalysts* **2020**, *10*, 1038.
[58] A. Bansal, D. Kar, S. D. Pandey, A. Matcha, N. G. Kumar, S. Nathan, A. S. Ghosh, *Protein J.* **2017**, *36*, 220–227.
[59] T. Brun, J. Peduzzi, M. M. Canica, G. Paul, P. Névot, M. Barthélémy, R. Labia, *FEMS Microbiol. Lett.* **1994**, *120*, 111–117.
[60] SAINT, version 6.45, Bruker Analytical X-ray Systems, Madison, 2003.
[61] G. M. Sheldrick SADABS Program for Absorption Correction, version 2.10, Analytical X-ray Systems, Madison, 2003.
[62] a) G. M. Sheldrick, A *cta Crystallogr. Sect. C Struct. Chem.* **2015**, *71*, 3–8; b) G. M. Sheldrick, *Acta Crystallogr. A.* **2008**, *64*, 112–22; c) SHELXTL-2013/4, Bruker Analytical X-ray Instruments, Madison, WI, **2013**.
[63] a) A. L. Spek, *Acta Crystallogr. Sect. C Struct. Chem.* **2015**, *71*, 9–18; b) A. L. Spek, *Acta Crystallogr. Sect. D Biol. Crystallogr.* **2009**, *65*, 148–155.
[64] L. J. Farrugia, *J. Appl. Crystallogr.* **1999**, *32*, 837–838.
[65] C. Palmer, D. CRYSTAL MAKER, Cambridge University Technical Services, 1996.
[66] O. Trott, A. J. Olson, *J. Comput. Chem.* **2010**, *31*, 455–461.
[67] Gaussian 16, Revision C.01, M. J. Frisch, G. W. Trucks, H. B. Schlegel, G. E. Scuseria, M. A. Robb, J. R. Cheeseman, G. Scalmani, V. Barone, G. A. Petersson, H. Nakatsuji, X. Li, M. Caricato, A. V. Marenich, J. Bloino, B. G. Janesko, R. Gomperts, B. Mennucci, H. P. Hratchian, J. V. Ortiz, A. F. Izmaylov, J. L. Sonnenberg, D. Williams-Young, F. Ding, F. Lipparini, F. Egidi, J. Goings, B. Peng, A. Petrone, T. Henderson, D. Ranasinghe, V. G. Zakrzewski, J. Gao, N. Rega, G. Zheng, W. Liang, M. Hada, M. Ehara, K. Toyota, R. Fukuda, J. Hasegawa, M. Ishida, T. Nakajima, Y. Honda, O. Kitao, H. Nakai, T. Vreven, K. Throssell, J. A. Montgomery, Jr., J. E. Peralta, F. Ogliaro, M. J. Bearpark, J. J. Heyd, E. N. Brothers, K. N. Kudin, V. N. Staroverov, T. A. Keith, R. Kobayashi, J. Normand, K. Raghavachari, A. P. Rendell, J. C. Burant, S. S. Iyengar, J. Tomasi, M. Cossi, J. M. Millam, M. Klene, C. Adamo, R. Cammi, J. W. Ochterski, R. L. Martin, K. Morokuma, O. Farkas, J. B. Foresman, D. J. Fox, Gaussian, Inc., Wallingford CT, **2016**.
[68] C. Lee, W. Yang, R. G. Parr, *Phys. Rev. B* **1988**, *37*, 785–789.
[69] A. D. Becke, *J. Chem. Phys.* **1993**, *98*, 5648–5652.
[70] S. Grimme, J. Antony, S. Ehrlich, H. Krieg, *J. Chem. Phys.* **2010**, *132*, 154104.
[71] W. R. Wadt, P. J. Hay, *J. Chem. Phys.* **1985**, *82*, 284–298.
[72] A. V. Marenich, C. J. Cramer, D. G. Truhlar, *J. Phys. Chem. B* **2009**, *113*, 6378–6396.
[73] K. Fukui, *Acc. Chem. Res.* **1981**, *14*, 363–368.

Manuscript received: April 27, 2023
Accepted manuscript online: June 6, 2023
Version of record online: June 6, 2023